

## Spin-Glass Behavior of Amorphous $\text{Co}_2\text{Ge}$ Synthesized by Mechanical Milling

G. F. Zhou and H. Bakker

*Van der Waals-Zeeman Laboratorium, Universiteit van Amsterdam, Valckenierstraat 65, 1018 XE Amsterdam, The Netherlands*

(Received 22 November 1993)

Amorphous  $\text{Co}_2\text{Ge}$  was synthesized by ball milling crystalline  $\text{Co}_2\text{Ge}$ , a state which cannot be obtained by traditional rapid solidification. It exhibits a single transition from the paramagnetic to the spin-glass state at 41 K ( $T_f$ ) as defined by a sharp asymmetric cusp in the lowest field ac susceptibility. In fields  $\geq 30$  Oe the cusp in both ac and dc susceptibility curves becomes a rounded maximum and  $T_f$  decreases. Below  $T_f$  the magnetization reveals thermal hysteresis. Using the Sherrington-Kirkpatrick theory the spin-glass order parameter is derived and a spin-glass phase was synthesized by mechanical milling. This phase can be described by mean-field theory.

PACS numbers: 75.30.Cr, 75.30.Kz, 75.50.Kj, 75.60.Ej

A spin glass is a particular type of magnetic alloy. The term "spin glass" is coined to describe the metastable magnetic state at low temperatures in some simple solid solutions, for example,  $\text{Au}_{1-x}\text{Fe}_x$  or  $\text{Cu}_{1-x}\text{Mn}_x$ , with  $x$  in the range  $10^{-3}$  to  $10^{-1}$  [1,2]. In the spin-glass phase, magnetic moments are frozen into equilibrium orientations, but there is no long-range order. It is well established that a sharp maximum in susceptibility in low fields and its peculiar sensitivity to the external field are good indications for a spin glass [3,4]. It was suggested that the transition from paramagnet to spin glass is a second-order transition [5-7]. To detect the presence of such a state the order parameter,  $q$ , was introduced. Among all the spin-glass alloys discovered up until now, most of them are dilute solid solutions with a rather low content of the magnetic element (usually a few atomic percent). There are some examples of alloys showing spin-glass behavior and having a content of magnetic elements as high as 70 at.%. However, these alloys are composed of at least two transition metals and at least two nontransition elements in order to obtain the appropriate degrees of ferromagnetic and antiferromagnetic exchange. Examples are amorphous  $(\text{Fe}_x\text{Ni}_{1-x})_{79}\text{P}_{13}\text{B}_8$  and  $(\text{Fe}_x\text{Ni}_{1-x})_{75}\text{P}_{16}\text{B}_6\text{Al}_3$  [4]. Moreover, most of them exhibit multitransitions from the paramagnetic to the ferromagnetic state and subsequently to the spin-glass state (reentry behavior).

In this Letter, we report a new type of spin-glass material with a very high content of the magnetic element, namely, amorphous  $\text{Co}_2\text{Ge}$  synthesized by mechanical milling of the crystalline intermetallic compound  $\text{Co}_2\text{Ge}$ . This binary alloy shows a single transition from the paramagnetic to the spin-glass state. To our best knowledge this is the first report of the preparation of a spin glass by mechanical milling. Moreover, the material shows "pure" spin-glass behavior, is a binary alloy with a high content of the magnetic element (67 at.%), and is in the amorphous state. Amorphous  $\text{Co}_2\text{Ge}$  cannot be obtained by traditional melt spinning. Therefore, mechanical milling turns out to be a unique technique to obtain the material

in this special state.

Crystalline  $\text{Co}_2\text{Ge}$  was obtained by arc melting of weighed amounts of pure cobalt and germanium in a purified argon atmosphere and by subsequent annealing at 673-773 K for a few days. The mechanical milling was carried out in a hardened steel vial with a vacuum of about  $10^{-6}$  Torr. The melt-spinning technique was used to quench  $\text{Co}_2\text{Ge}$  from the liquid state to room temperature. High-frequency melting was used. The cooling rate was about  $10^7$  K per second. X-ray diffraction patterns were taken at room temperature by means of a Philips diffractometer with vertical goniometer using  $\text{Cu } K\alpha$  radiation. The ac susceptibility measurements were performed from room temperature to liquid helium temperature in self-constructed equipment. In this apparatus the sample is mounted in a secondary coil which is connected in series with a counterwound identical coil. The two coils are placed in a primary coil which generates an ac magnetic field. A voltage is induced over the secondary coil by mutual inductance which is monitored by a lock-in amplifier. A reference signal is supplied to the lock-in amplifier by a voltage generated by the ac current of the primary coil over a given resistor. Theoretically, the signal over the secondary coil is zero if there is no sample in one of the coils. The coil system with the sample is mounted in a sample chamber, which contains a thermometer and a heater in order to control the temperature. The sample chamber is separated by an exchange chamber from liquid helium. The cooling of the sample is controlled by the amount of helium gas in the exchange chamber. The low dc field magnetization was measured in a self-designed magnetometer. The sensitivity of the magnetometer is better than  $10^{-5}$   $\text{A m}^2$ .

The starting compound  $\text{Co}_2\text{Ge}$  has the orthorhombic structure ( $\text{Co}_2\text{Si}$  type) with space group  $Pnma$  as can be found from the x-ray diffraction pattern (0 h) shown in Fig. 1. After ball milling, the crystalline compound transforms to the amorphous state. It was found from x-ray diffraction, differential scanning calorimetry (DSC), and magnetic measurements that the amorphiza-

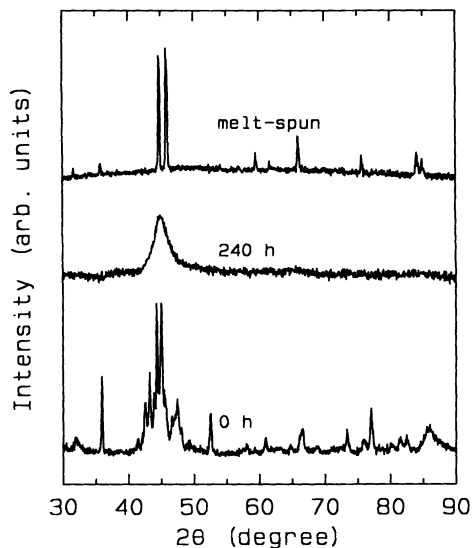


FIG. 1. X-ray diffraction patterns of  $\text{Co}_2\text{Ge}$  as-prepared (0 h), after 240 h of milling and of a melt-spun sample.

tion starts at a milling time of 80 h and is complete after milling for 240 h. (The details of the structural evolution are presented elsewhere [8].) In Fig. 1 the x-ray diffraction pattern of  $\text{Co}_2\text{Ge}$  after 240 h of milling is given as the central curve labeled 240 h. It shows the typical characteristics of an amorphous phase. The x-ray diffraction pattern of  $\text{Co}_2\text{Ge}$  rapidly quenched from the liquid state is also given in Fig. 1 as the top curve labeled melt spun. It is clear that the pattern of the melt-spun  $\text{Co}_2\text{Ge}$  is characteristic of a crystalline phase with hexagonal structure ( $\text{Ni}_2\text{In}$  type with space group  $P6_3/mmc$ ), which exists at higher temperature in the phase diagram [9]. Apparently, no amorphous phase is formed by traditional rapid solidification. This is confirmed by DSC analysis and magnetic measurements. All samples milled for 240 h or longer exhibit the same physical properties. Therefore, we will present the results of the sample milled for 240 h as representative of the amorphous material.

Both the as-prepared and melt-spun crystalline  $\text{Co}_2\text{Ge}$  are ferromagnets at lower temperatures. Values of the paramagnetic Curie temperature and the effective magnetic moment of crystalline and amorphous  $\text{Co}_2\text{Ge}$  are given in Table I. These were derived from the high-field magnetic susceptibility in the temperature range from 50 K to room temperature by the Curie-Weiss law. The ferromagnetic Curie temperatures for the crystalline material obtained from both ac-susceptibility measurements and Arrot plots are also tabulated in Table I. The paramagnetic Curie temperature of amorphous  $\text{Co}_2\text{Ge}$  is also positive, indicating that in amorphous  $\text{Co}_2\text{Ge}$  the dominant exchange interactions are ferromagnetic. The effective magnetic moment per Co atom in the amorphous state is larger than twice the value in the crystalline state. The slope of the inverse susceptibility decreases gradually with decreasing temperature as can be found from Figs.

TABLE I. The effective magnetic moment  $p_{\text{eff}}$  [ $\mu_B/(\text{Co atom})$ ], the paramagnetic Curie temperature  $\theta_p$  (K), the ferromagnetic Curie temperature  $T_C$  (K), and freezing temperature  $T_f$  (K) of as-prepared  $\text{Co}_2\text{Ge}$ , amorphous  $\text{Co}_2\text{Ge}$ , and melt-spun  $\text{Co}_2\text{Ge}$ .

Sample	$p_{\text{eff}}$ [ $\mu_B/(\text{Co atom})$ ]	$\theta_p$ (K)	$T_C^{\text{ac}}$ (K)	$T_C^{\text{dc}}$ (K)	$T_f$ (K)
As-prepared $\text{Co}_2\text{Ge}$	1.29	56.3	46.4	47	...
Amorphous $\text{Co}_2\text{Ge}$	2.66	61.7	...	...	41
Melt-spun $\text{Co}_2\text{Ge}$	1.25	19.2	5	5	...

2 and 3. Both these observations are consistent with the "superparamagnetic" behavior observed in alloy spin glasses [1,4] and usually these effects are attributed to the formation of stable clusters of spins, locked together by the stronger exchange interactions. This causes a decrease of the average value of the remaining exchange interactions.

The temperature dependence of the ac susceptibility (the real part) of amorphous  $\text{Co}_2\text{Ge}$  in different fields measured at a frequency  $\nu$  of 109 Hz is displayed in Fig. 2. The values are normalized by the applied fields. This figure exhibits the following characteristics: (i) A very sharp cusp at about 41 K is observed when the applied field is low but this cusp loses its sharpness and becomes a broad maximum with increasing external field. When the applied field is increased to 90 Oe even no maximum is observable in the temperature range, where the measurements were performed. (ii) Both the height of the cusp and the peak temperature decrease with increasing applied field. These phenomena are very similar to those observed by Cannella and Mydosh in the typical alloy spin-glass AuFe [1]. In addition, a pronounced anomaly in the imaginary part  $\chi''$  of the ac susceptibility is ob-

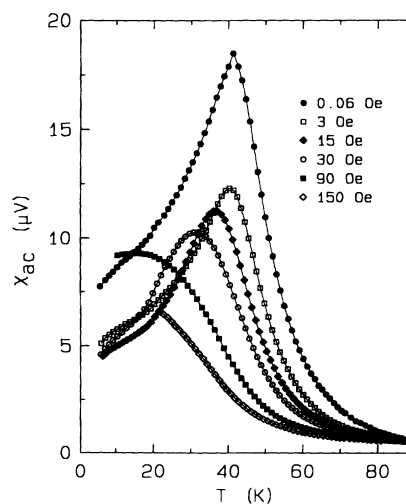


FIG. 2. Temperature dependence of the ac susceptibility (the real part) of amorphous  $\text{Co}_2\text{Ge}$  in different ac fields. A frequency of 109 Hz was used.

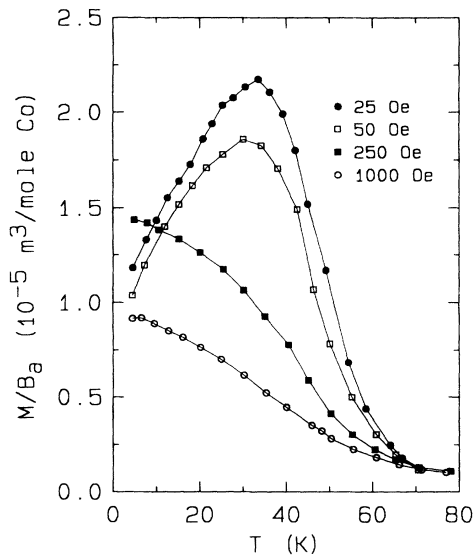


FIG. 3.  $M/B_a$  vs  $T$  curves for amorphous  $\text{Co}_2\text{Ge}$  measured in various dc magnetic fields after zero-field cooling (ZFC).

served around the freezing temperature. The maximum in  $|d\chi''(T)/dT|$  nicely coincides with the maximum in the real part, i.e., at the freezing temperature  $T_f(\nu)$ . The appearance of the imaginary component means that relaxation processes are affecting the measurement and that decoupling of spins causes energy absorption. A similar behavior of  $\chi''$  around  $T_f$  was observed in alloy spin glasses [4]. Because of the heating effect by eddy currents during the measurement, the temperature of the sample cannot reach lower values when the applied field is larger than 90 Oe. The influence of the frequency in the range of 14 to 109 Hz on the cusp in ac susceptibility was also investigated. It turned out that with increasing frequency, the freezing temperature slightly increased with a value  $\Delta T_f/[T_f \Delta \ln \nu] = 0.04$ , while the cusp became somewhat rounded. This is also observed in other spin glasses [4].

Low dc field magnetization measurements confirmed the results obtained by measurements of the ac susceptibility. Figure 3 shows  $M/B_a$  as a function of temperature for amorphous  $\text{Co}_2\text{Ge}$  in different external fields. When the applied fields are small so that the magnetization is proportional to susceptibility,  $M/B_a$  gives the initial dc susceptibility  $\chi$ . After zero-field cooling, the measurements were performed with increasing temperature. A sharp maximum similar to that in the ac susceptibility is evident, when measuring in a field of 25 Oe. With increasing field this maximum becomes a rounded transition and disappears when the field is high, i.e., in a field as large as 250 Oe. This maximum also shifts to lower temperature with increasing field. The value of  $M/B_a$  also decreases with increasing field. These results fully confirm the results of the ac susceptibility.

Irreversibility is a characteristic of spin glasses. The magnetic behavior differs depending on whether the ma-

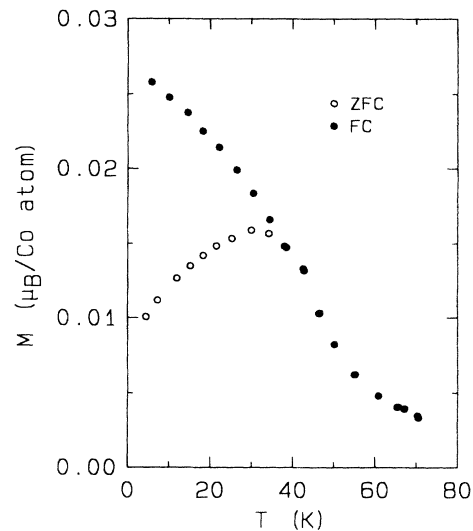


FIG. 4. Temperature dependence of the magnetization of amorphous  $\text{Co}_2\text{Ge}$  after zero-field cooling (ZFC) and field cooling (FC) measured in a field of 50 Oe.

terial is cooled down with or without field. This is illustrated by Fig. 4. This figure shows the  $M$  vs  $T$  curves of amorphous  $\text{Co}_2\text{Ge}$  after zero-field cooling (ZFC) and field cooling (FC) in a field of 50 Oe. This figure nicely illustrates the different temperature behavior between FC and ZFC. Remarkable are the features at  $T_f$ . The FC magnetization decreases gradually with increasing temperature but is virtually independent of time: During an arrest at a given temperature ( $T < T_f$ ), the magnetization remains unchanged. Furthermore, the process of FC followed by field warming is reversible. When we cycled the temperature back and forth (with  $B = \text{const}$ ) the FC magnetization traced the same path. On the other hand, the ZFC magnetization is zero until the field is applied. In the presence of the external field, the magnetization increases with increasing temperature until  $T_f$ , where the two curves coincide (open circles). These traces are irreversible. This means that  $M_{ZFC}$  is always drifting upwards. When we continued to increase the temperature above  $T_f$  and then cooled the sample back down, first above  $T_f$  the reversible "paramagnetic" regime was observed and subsequently by further cooling the magnetization became the reversible  $M_{FC}$ . So, the dc field, when applied below  $T_f$ , creates a metastable and irreversible state in amorphous  $\text{Co}_2\text{Ge}$ . Moreover, the temperature where both curves coincide is shifted to lower values with increasing measuring field. Figure 5 shows the field dependence of the magnetization of amorphous  $\text{Co}_2\text{Ge}$  after ZFC and FC in a field of 1 T at 4.4 K. The FC curve is clearly displaced relative to the ZFC curve. There is a remanence of approximately  $0.09\mu_B/(\text{Co atom})$ . No remanence is observed after zero-field cooling within the experimental accuracy. The two curves coincide at a field of 0.6 T. By extrapolating the magnetization curve to zero field, the magnetic moment of Co is found to be

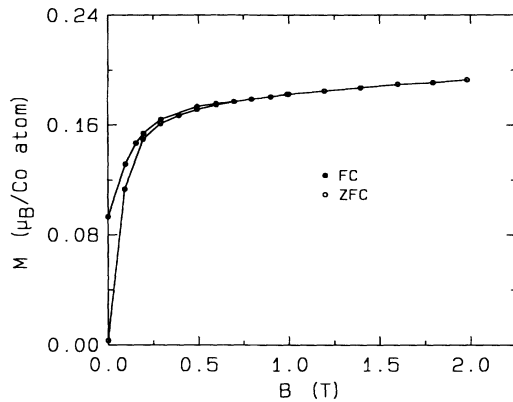


FIG. 5. Field dependence of the magnetization of amorphous  $\text{Co}_2\text{Ge}$  after zero-field cooling (ZFC) and field cooling (FC) measured at 4.4 K.

equal to  $0.17\mu_B$  per Co atom. All together the results shown above prove that amorphous  $\text{Co}_2\text{Ge}$  undergoes, upon cooling from room temperature to lower temperature, a single paramagnetic to spin-glass (SG) transition at about 41 K (the freezing temperature,  $T_f$ ) rather than a paraferromagnetic transition. The freezing temperature is shifted to lower values by increasing the magnitude of the applied magnetic field.

The susceptibility  $\chi$  provides an experimental probe of the spin-glass order parameter  $q$ , since [7]

$$\chi(T) = C(T)[1 - q(T)]\{T - \theta(T)[1 - q(T)]\}^{-1}, \quad (1)$$

where both  $C(T)$  and  $\theta(T)$  are temperature independent in the mean-field theory used in Ref. [7] and should be slowly varying close to the spin-glass transition temperature in real materials. Since  $q$  vanishes for  $T \geq T_f$ , Eq. (1) predicts an asymmetry in the temperature dependence above and below  $T_f$ . The behavior of the susceptibility in fields below 30 Oe is consistent with a second-order transition. For the evaluation of the order parameter,  $\chi_{ac}(T)^{-1}$  obtained in the lowest field (0.06 Oe, Fig. 2) was extrapolated. In this way the intercept  $\theta(T_f)$  and the slope  $C(T_f)$  and from these, using Eq. (1)  $q(T)$  was found:

$$q(T) \approx 1 - T\chi(T) [C(T_f) + \theta(T_f)\chi(T)]^{-1}. \quad (2)$$

The values of  $q(T)$  derived by Eq. (2) are shown in Fig. 6. It is clear that the measured  $q(T)$  almost linearly increases with decreasing temperature. Graphical analysis of the data in Fig. 6, using  $T_f = 41$  K, shows a power law for  $q(T)$ , i.e.,  $q(T) \propto (T_f - T)^\beta$ , with a  $\beta$  value of about 0.95. Thus the temperature dependence of  $q$ , as shown in Fig. 6, is in agreement with the prediction by mean-field theory.

This value does not agree with the percolation prediction, where  $\beta$  is known to be equal to  $0.39 \pm 0.01$  in three dimensions [10].

In conclusion, the amorphous phase of  $\text{Co}_2\text{Ge}$  has

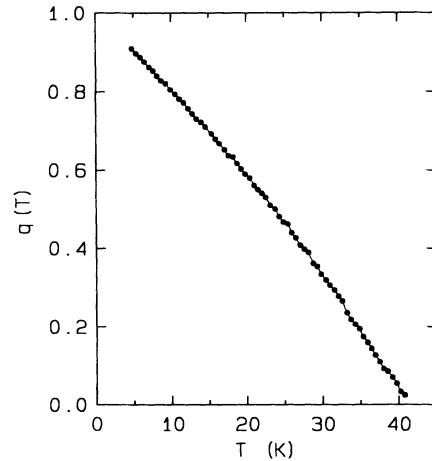


FIG. 6. Spin-glass order parameter,  $q(T)$ , derived from the data of the inverse susceptibility using Eq. (2).

been successfully synthesized by mechanical milling of the crystalline intermetallic compound  $\text{Co}_2\text{Ge}$ . Amorphous  $\text{Co}_2\text{Ge}$  cannot be obtained by the traditional rapid solidification method. The material shows a single transition from the paramagnetic to the spin-glass state below 41 K. The spin-glass transition temperature is very sensitive to the external field. The susceptibility is described well by the Sherrington-Kirkpatrick theory. The spin-glass order parameter is deduced. It turned out that this "spin-glass" phase is described well by the mean-field theory. It must be emphasized that  $\text{Co}_2\text{Ge}$  represents the first example of the use of mechanical milling to synthesize spin glasses. We believe that there are more alloy systems that could be driven to the spin-glass state by high-energy ball milling, in particular in cases where spin-glass states cannot be obtained by traditional rapid solidification.

The financial support by the Dutch Foundation for Fundamental Research on Matter (FOM) is gratefully acknowledged.

- [1] V. Cannella and J.A. Mydosh, *Phys. Rev. B* **6**, 4220 (1972).
- [2] J.A. Mydosh and V. Cannella, in *Ferromagnetic Materials*, edited by E.P. Wohlfarth (North-Holland, Amsterdam, 1980), Vol. 1, p. 71.
- [3] P.A. Beck, *Prog. Mater. Sci.* **23**, 1 (1978).
- [4] J.A. Mydosh, in *Spin Glasses: An Experimental Introduction* (Taylor & Francis, London, 1993).
- [5] K.H. Fischer, *Phys. Rev. Lett.* **34**, 1438 (1975).
- [6] S.F. Edwards and P.W. Anderson, *J. Phys. F* **5**, 965 (1975).
- [7] D. Sherrington and S. Kirkpatrick, *Phys. Rev. Lett.* **35**, 1792 (1975).
- [8] G.F. Zhou and H. Bakker (to be published).
- [9] T.B. Massalski, in *Binary Alloy Phase Diagrams* (American Society for Metals, Metals Park, OH, 1986), p. 768.
- [10] S. Kirkpatrick, *Phys. Rev. Lett.* **36**, 17 (1976).